

SHORT COMMUNICATION **OPEN ACCESS**

Extracellular Vesicle-Mediated Delivery of 20S Proteasomes Enhances Tau Degradation in Recipient Cells

Jiseong Kim^{1,2}  | Yuping Zhao³  | Hyun Young Kim^{4,5}  | Sumin Kim^{1,2}  | Yanxialei Jiang³  | Min Jae Lee^{1,2,6} 

¹Department of Biochemistry and Molecular Biology, Seoul National University College of Medicine, Seoul, South Korea | ²Department of Biomedical Sciences, Seoul National University Graduate School, Seoul, South Korea | ³Shandong Provincial Key Laboratory of Tumor Imaging Equipment Development and Theragnostic Technologies, Linyi University, Linyi, China | ⁴Department of Oral Microbiology and Immunology, Dental Research Institute, School of Dentistry, Seoul National University, Seoul, South Korea | ⁵Department of Microbiology, ADA Forsyth Institute, Somerville, Massachusetts, USA | ⁶Ischemic/Hypoxic Disease Institute, Convergence Research Center for Dementia, Medical Research Center, Seoul National University, Seoul, South Korea

Correspondence: Yanxialei Jiang (jyxialei@lyu.edu.cn) | Min Jae Lee (minjlee@snu.ac.kr)

Received: 6 January 2025 | **Accepted:** 10 April 2025

Funding: This work was supported by grants from the National Research Foundation (NRF) of Korea (2020R1A5A1019023, RS-2021-NR059245 and RS-2023-00261784 to M.J.L.; RS-2024-00410687 to J.K.; 2022R1C1C2007752 to H.Y.K.), the Korea Health Industry Development Institute and Korea Dementia Research Centre (RS-2024-00332875 to M.J.L.) and the China Scholarship Council (202108370145 to Y.J.).

Keywords: degradation | delivery | extracellular vesicle | proteasome | tau

ABSTRACT

The 26S proteasome holoenzyme comprises 20S catalytic and 19S regulatory complexes. Accumulating evidence suggests that the majority of proteasomes in the extracellular space exist as free 20S proteasomes; however, their origin and pathophysiological function remain to be determined. Here, we report that cellular proteasomes are effectively packaged into the lumen of extracellular vesicles (EVs) and secreted in a structurally intact and enzymatically active 20S form. We further demonstrate that EV-encapsulated 20S proteasomes are delivered to recipient cells and facilitate the degradation of overexpressed tau proteins without disrupting global proteolytic pathways. These findings highlight a novel cell-to-cell communication system that transports the proteasomes to target cells for the clearance of proteotoxic substrates. Further characterisation of this homeostatic mechanism will improve our understanding of organismal stress response mechanisms and may provide a therapeutic approach to treat various proteinopathies, including Alzheimer's disease.

1 | Introduction

The major ATP-dependent proteolytic enzyme in eukaryotic cells is the 26S proteasome (Finley et al. 2016; Turker et al. 2021). This holoenzyme is formed by a non-covalent interaction of a catalytic 20S proteasome (~730 kDa) and one or two 19S regulatory complexes (~930 kDa). The heptameric PSMA/ α ring of the 20S and the hexameric PSMC/Rpt ATPase ring of the 19S form an asymmetric interface, generating a continuous axial channel for

substrate translocation into the catalytic chamber (Matyskiela et al. 2013; Sledz et al. 2013). The 19S processes are driven by ATP hydrolysis, but the 20S proteolysis by the active PSMB/ β subunits (threonine proteases) does not require energy. Recent studies reveal that over half of proteasomes in mammalian cells exist as free 20S forms (Fabre et al. 2014), which were initially considered as a latent enzyme or assembly intermediate. The physiological importance of ubiquitin-independent, 20S-mediated proteolysis is gaining recognition, especially in connection with the

Jiseong Kim and Yuping Zhao contributed equally to this work.

This is an open access article under the terms of the [Creative Commons Attribution-NonCommercial](https://creativecommons.org/licenses/by-nc/4.0/) License, which permits use, distribution and reproduction in any medium, provided the original work is properly cited and is not used for commercial purposes.

© 2025 The Author(s). *Journal of Extracellular Vesicles* published by Wiley Periodicals LLC on behalf of International Society for Extracellular Vesicles.

degradation of oxidised and intrinsically disordered proteins (Abi Habib et al. 2020; Choi et al. 2023).

In addition to intracellular proteasomes, extracellular proteasomes in the circulatory system (c-proteasomes) have been intensively investigated, and their concentration and proteolytic activity have been linked to disease severity and patient prognosis (Choi et al. 2021; Dwivedi et al. 2021; Ben-Nissan et al. 2022). However, some of the reported findings are inconsistent and contradictory, possibly due to a lack of standardised methodology. Nevertheless, c-proteasomes purified from human serum or plasma using either chromatography or ultracentrifugation appear to be free 20S forms, lacking the 19S subcomplex (Rajkumar et al. 2014; Wu et al. 2020; Kostallari et al. 2021). Although the precise configuration of c-proteasomes has yet to be determined, given the ATP-depleted environment of multicellular organisms' extracellular milieu, the presence of c-proteasomes circulating as a 20S form seems plausible.

Cells continuously release a variety of extracellular vesicles (EVs), including exosomes and ectosomes, into the surrounding extracellular space. Exosomes are formed from multivesicular bodies and secreted via exocytosis, whereas ectosomes originate from the plasma membrane (Mathieu et al. 2021). Despite their distinct biogenesis, these two classes of EVs essentially mediate long-distance intercellular communication by delivering macromolecules such as proteins, nucleic acids and lipids to diverse tissues and organs, thereby affecting the biological functions of recipient cells (Rackov et al. 2018; Mathieu et al. 2019). Owing to their intrinsic biocompatibility and ability to penetrate plasma membranes, EVs offer advantages as delivery vehicles over polymeric nanoparticles, dendrimers, micelles and liposomes and have been shown to carry a variety of cargoes in vivo (Herrmann et al. 2021; Murphy et al. 2021; Piffoux et al. 2017; EL Andaloussi et al. 2013). Encapsulating pharmacological agents, whether small-molecule drugs or enzymes, in EVs can also preserve their potency/activity, lengthen circulation time and improve their ability to cross biological barriers, such as the blood-brain barrier.

In this study, we report that 20S proteasomes are effectively loaded into the lumen of EVs while maintaining their structural integrity and proteolytic activity. This will be the first instance demonstrating that EVs containing 20S proteasomes can be effectively internalised into several cell lines, aiding the degradation of overexpressed tau proteins. These findings suggest that 20S proteasome delivery via EVs may be an essential mechanism for organisms to respond to proteotoxic stressors. Furthermore, our findings highlight the potential of the EV-based 20S proteasome delivery system as a novel therapeutic approach for proteotoxic diseases.

2 | Materials and Methods

2.1 | Antibodies and Reagents

Antibodies for immunoblotting used in this study were as follows: anti- β -actin/ACTB (A1978; Merck), anti-TSG101 (ab125011; Abcam), anti-Alix (2171S; Cell Signaling Technology), anti-CD63 (ab134045; Abcam), anti-Calnexin (A303-694A; BETHYL), anti-

Fibronectin (F3648; Sigma), anti-PSMA4 (PW8115; Enzo Life Science), anti-PSMA2 (PW8105; Enzo Life Science), anti-His (MA121315; Invitrogen), anti-PSMB2 (SC-54676; Santa Cruz), anti-PSMB6 (PA1-978; Invitrogen), anti-PSMC4 (AT3466a; Abgent), anti-PSMC2 (sc-166972; Santa Cruz), anti-PSMD1 (sc-514809; Santa Cruz), anti-20S MCP231 (sc-58412; Santa Cruz), anti-GFP (sc-9996; Santa Cruz), anti-Ub clone P4D1 (sc-8017; Santa Cruz), anti-Tau (AHB0042; Invitrogen), anti-Nrf2 (ab62352; Abcam), anti-p53 (MA5-12557; Invitrogen), anti-Mcl-1 (94296S; Cell Signaling Technology), anti-LAMP2 (Ab18528; Abcam), anti-LAMP1 (PA1-654A; Invitrogen), anti-Rab7 (D95F2; Cell Signaling Technology), anti-p62 (ab56416; Abcam) and anti-LC3B (L7534; Sigma). Secondary antibodies for immunoblotting (horseradish peroxidase [HRP]-conjugated anti-mouse IgG and anti-rabbit IgG antibodies) and for immunostaining (goat anti-rabbit Alexa Fluor 594 IgG and goat anti-mouse Alexa Fluor 488 IgG antibodies) were purchased from Merck and Invitrogen, respectively. The proteasome inhibitors were MG132 (M-1157; AG Scientific) and bortezomib (A2614; Apexbio). The fluorogenic peptide substrate suc-LLVY-AMC (I-1395) was purchased from Bachem. Doxycycline was obtained from Biosesang (D1121) and ATP γ S was purchased from Jena Bioscience (NU-406).

2.2 | Cell Culture

HEK293-PSMB2/ β 4-HB and HEK293-TREX-htau40 cell lines were generated as previously described (Choi et al. 2023). Briefly, cells were cultured in DMEM medium containing 10% foetal bovine serum (FBS) and 100 U/mL penicillin-streptomycin at 37°C in a 5% CO₂ incubator. A549 and SW480 cells were cultured in RPMI 1640 and Leibovitz's L-15 media, respectively. We used FBS-deprived media 24 h before EV isolation to exclude free c-proteasomes, nanovesicles and protein aggregates in serum (Lehrich et al. 2021; Gardiner et al. 2016; Rider et al. 2016).

2.3 | Isolation of EVs

The isolation of EVs from the cell culture supernatant was optimised using ultracentrifugation as previously reported (Patel et al. 2019; Théry et al. 2018; Lobb et al. 2015). The conditioned medium (FBS-depleted) was collected and differentially centrifuged at 300 \times g for 10 min, 2000 \times g for 10 min and 10,000 \times g for 30 min. The concentrated supernatant was ultracentrifuged at 120,000 \times g for 3 h at 4°C using an Optima XE-100 Ultracentrifuge with a 45 Ti rotor (Beckman Coulter). The pellet was then gently resuspended in PBS before being ultracentrifuged at 120,000 \times g for 2 h at 4°C in the Optima Ultracentrifuge with a 41 Ti rotor (Beckman Coulter). The protein concentration of the isolated EVs was determined using a BCA Protein Assay Kit (P8100-050; GenDEPOT) following the manufacturer's instructions. Isolated EVs were aliquoted, immediately frozen with liquid nitrogen and stored at -80°C.

2.4 | Transmission Electron Microscopy (TEM)

EV samples were negatively stained as previously described (Lim et al. 2023). Briefly, five microliters of each EV sample were loaded onto a glow-discharged formvar/carbon-coated copper grid

(Electron Microscopy Sciences) and incubated at room temperature for 1 min. The samples were then washed twice with distilled water and stained with 2% uranyl acetate for 1 min. The negatively stained EV images were captured using an electron microscope (LIBRA 120, Zeiss Microscopy) with a 120 kV acceleration.

2.5 | Nanoparticle Tracking Analysis

The size and concentration of EVs were determined using the NanoSight LM10 (Malvern Instruments) as previously reported (Lim et al. 2023). To obtain the desired concentration range, all samples were diluted in PBS to a final volume of 500 μ L. The following settings were used: screen gain 12, camera level 15 and detection threshold 3.

2.6 | Measurement of Proteasomal Proteolytic Activity

Hydrolysis of the fluorogenic peptide suc-LLVY-AMC was assessed to determine the proteolytic activity of purified 26S and 20S encapsulated within the isolated EVs, as previously described (Choi et al. 2016). Briefly, 5 nM of purified proteasomes or a predetermined amount of EVs and 12.5 μ M of suc-LLVY-AMC were added to the assay buffer (50 mM Tris-HCl pH 7.5, 1 mg/mL BSA, 1 mM EDTA, 1 mM ATP and 1 mM DTT). The levels of AMC hydrolysed by proteasomes were determined by measuring free AMC fluorescence in a black 96-well plate every 3 min at 380 nm excitation and 460 nm emission wavelengths using a Tecan Infinite M200 fluorometer.

2.7 | Native Gel Electrophoresis and In-Gel Activity Assay

The isolated EVs and cell lysates were prepared in a lysis buffer (25 mM Tris-HCl [pH 7.5], 10% glycerol [v/v], 5 mM $MgCl_2$, 1 mM ATP, 1 mM DTT and a protease inhibitor cocktail). The samples were resolved using NuPAGE 3%–8% Tris-Acetate Protein Gels (EA03755; ThermoFisher) at 150 V for 4 h. The gels were then incubated in an in-gel activity buffer (20 mM Tris-HCl, 1 mM ATP, 5 mM $MgCl_2$) containing proteasome substrate (100 μ M suc-LLVY-AMC) for 10 min to visualise the separated proteasome complexes. To activate and visualise the 20S proteasome, the gel was incubated in the in-gel activity buffer containing 0.02% SDS. Following the in-gel activity assay, the gel was transferred to PVDF membranes for immunoblot analysis (Byun et al. 2023).

2.8 | Cellular Uptake of EV-Proteasomes

Recipient cells, such as A549, SW480 and HEK293 cells, were cultured in 6-well plates, washed with PBS at ~95% confluency and treated with varying amounts of isolated EVs for 24 h. For SDS-PAGE, cells were then washed twice with PBS and lysed in RIPA buffer (150 mM NaCl, 0.5% sodium deoxycholate, 0.1% SDS, 1% NP-40, 50 mM Tris-HCl [pH 8.0]) supplemented with a protease inhibitor cocktail and phosphatase inhibitor sodium as supernatants. Whole-cell lysates (WCLs) were collected after centrifugation at 14,000 \times g for 30 min at 4°C. WCLs

were mixed with 5 \times SDS sample buffer (final 10% glycerol, 2% SDS, 0.05% bromophenol blue, 50 mM Tris-HCl [pH 6.8] and 5% 2-mercaptoethanol) and denatured at 85°C for 10 min. Proteins were separated by SDS-PAGE and transferred to a 0.45 μ m polyvinylidene difluoride membrane for subsequent immunoblotting analysis.

2.9 | Immunofluorescence Staining (IFS)

Cells were cultured on coverslips in 24-well plates. After treating 20 μ g/mL of isolated EVs for 24 h, the cells were fixed with 4% paraformaldehyde for 15 min at room temperature (RT) and washed three times with PBS. Cells were permeabilised with 0.5% (v/v) Triton X-100 (0005-00579; Daejung Chemicals) in PBS for 15 min before being washed three times with PBS for 5 min each. The cells were then blocked with 2% bovine serum albumin (BSA; Bovogen) in PBS for 1 h at RT. Primary antibodies, diluted in 2% BSA in PBS, were applied to cells and incubated at 4°C overnight. The cells were then washed three times with PBS for 10 min each before incubating with Alexa Fluor-conjugated secondary antibodies diluted in 2% BSA in PBS, for 1 h at RT. Fluorescence microscopy was performed using coverslips mounted on glass slides using a DAPI-containing mounting solution (ab104139; Abcam). The images were captured using a fluorescent microscope (ECHO Revolve Hybrid).

2.10 | Statistical Analysis

The statistical significance of differences between groups was determined using the Student's *t*-test and one-way analysis of variance (ANOVA), followed by the Bonferroni post hoc test. Significant differences were defined as *p* values < 0.05.

3 | Results and Discussion

3.1 | EVs Isolated From the Serum-Free Media Contain Active Proteasomes

We previously demonstrated that c-proteasomes were present in human plasma as free 20S forms and that their activity decreased in patients with cognitive dysfunction (Yun et al. 2020). However, the secretory mechanisms supporting their functionality in an ATP-depleted environment, as well as the origin of c-proteasomes, remain unknown. We hypothesised that intracellular proteasomes were released into the extracellular fluid via EVs. To test this hypothesis, we first isolated EVs from the conditioned (serum-free) medium of HEK293-PSMB2/ β 4-HB cells (Byun et al. 2023), which stably overexpress the PSMB2 subunit of 20S proteasomes fused with a tandem hexahistidine-biotin (HB) tag through differential centrifugation (to exclude cells and debris) and ultracentrifugation (to precipitate EVs out of a vesicle-free supernatant; Figure S1A). The nanoparticle tracking analysis revealed that the final 120,000 \times g pellet contained highly homogenous EV particles with an average diameter of 136.3 ± 4.7 nm or 130.7 ± 5.2 nm, with or without trypsin (100 μ g/mL for 30 min), respectively (Figure 1A). TEM examination confirmed the presence of homogeneous nanoparticles in both the trypsin-treated and -untreated groups (Figure 1B), showing the

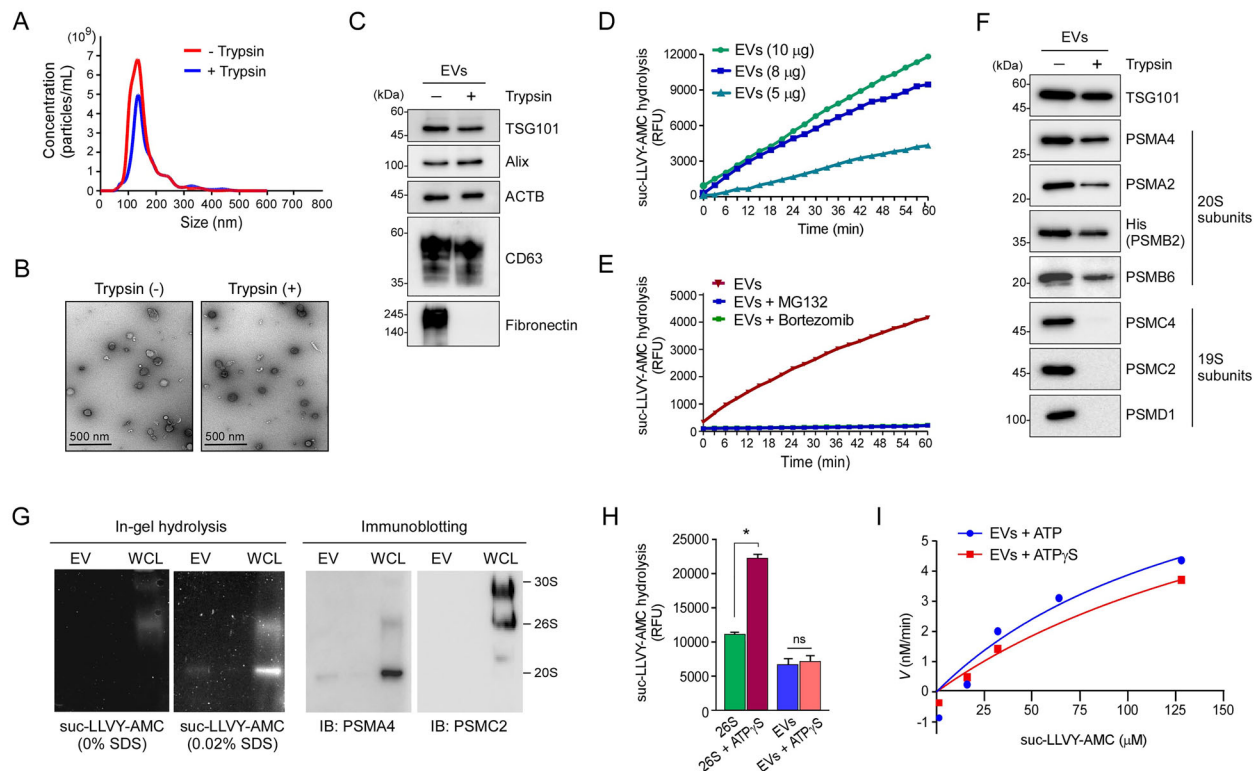


FIGURE 1 | Characterisation of isolated extracellular vesicles (EVs) and proteasomes encapsulated in EVs. (A) The EVs were isolated from HEK293-PSMB2/ β 4-HB cells and EV size distribution in both trypsinised (with 100 μ g/mL trypsin for 30 min at 37°C) and non-trypsinised samples (120,000 \times g pellets) was determined using nanoparticle tracking analysis (NTA). (B) Representative transmission electron microscopy (TEM) image of isolated EVs before and after trypsin treatment (100 μ g/mL for 30 min at 37°C). Scale bars = 500 nm. (C) Equal amounts of isolated EVs (2 μ g each) were analysed using denaturing sodium dodecyl sulphate-polyacrylamide gel electrophoresis (SDS-PAGE), followed by immunoblotting (IB) with the indicated antibodies. (D) Measurement of proteasome activity in 5, 8 and 10 μ g of isolated EVs using the suc-LLVY-AMC hydrolysis assay. Relative fluorescence units (RFU) were monitored every 3 min for over 1 h. (E) Proteasome activity in isolated EVs (4 μ g) in the presence or absence of proteasome inhibitors (20 μ M MG132 or 2 μ M bortezomib) was measured using the suc-LLVY-AMC hydrolysis assay. RFU, relative fluorescence unit. (F) Experiments were performed as described in (C) and 20S subunits were detected using antibodies against PSMA2, PSMA4, PSMB6 and His (PSMB2), while 19S subunits were detected using antibodies against PSMC2, PSMC4 and PSMD1. (G) Isolated EVs were resolved by non-denaturing (native) PAGE and then visualised using the in-gel suc-LLVY-AMC hydrolysis assay (left panels). Inactive 20S proteasomes were activated with 0.02% SDS (middle) and then subjected to immunoblotting analysis with anti-PSMA4 and PSMC2 antibodies (right). (H) Proteasome activity in purified 26S proteasomes (5 nM) and isolated EVs (5 μ g) was measured at the 60 min time point using the fluorogenic peptide suc-LLVY-AMC in the presence or absence of ATP γ S (1 mM). Data are presented as the mean \pm SD ($N = 3$); * $p < 0.05$, one-way ANOVA, followed by Bonferroni's post hoc test; ns, not significant. (I) Michaelis-Menten plot of EV-proteasomes with ATP γ S on concentration-dependent suc-LLVY-AMC cleavage for 30 min. The data were fit to a hyperbolic curve by nonlinear regression ($R^2 > 0.98$) to calculate the enzyme kinetic data. The graphs shown are representative of at least three independent determinations and each data point is the mean \pm SD ($N = 3$).

homogeneity and membrane integrity of enriched EVs, which were resistant to trypsin digestion.

To characterise the isolated EVs, we used well-established EV markers such as CD63 (a transmembrane protein; EV surface marker), TSG101 and Alix (cytosolic proteins; EV cargo markers) (Théry et al. 2018; Andreu and Yáñez-Mó 2014), which were detected by immunoblot analysis after denaturing sodium dodecyl sulphate-polyacrylamide gel electrophoresis (SDS-PAGE) (Figure 1C). We extensively treated the isolated EVs with trypsin (100 μ g/mL for 30 min at 37°C), which effectively removed fibronectin—an extracellular matrix protein often found on the surface of EVs—but had little effects on the other EV markers (Chanda et al. 2019; Choi, Go et al. 2020). To verify the presence of proteasomes in the EVs, we performed the suc-LLVY-AMC hydrolysis assay, which is a specific test for

chymotrypsin-like activity and also represents overall proteasome proteolytic activity (Kim et al. 2022). The isolated EVs showed significant proteasome activity that was highly dose- and time-dependent (Figure 1D). Moreover, the addition of the proteasome inhibitors MG132 (20 μ M) or bortezomib (2 μ M) to isolated EVs (4 μ g) effectively abolished the suc-LLVY-AMC signal (Figure 1E), indicating that the observed activity originated from the proteasomes within the EVs rather than other proteases in the EV cargo.

3.2 | Isolated EVs Contain Intact 20S Proteasomes

We then examined the proteasome subunits in the isolated EVs using SDS-PAGE/immunoblot analysis, which showed both 20S subunits (PSMA2/ α 2, PSMA4/ α 3 and PSMB6/ β 1) and 19S

subunits (PSMC2/Rpt1, PSMC4/Rpt3 and PSMD1/Rpn2) (Figure 1F). After 30 min of treatment with 100 µg/mL trypsin, all 19S subunits were completely digested, but the levels of 20S subunits and TSG101 decreased by less than 20%. To determine whether the residual 20S subunits after trypsinisation were due to their resistance to trypsin digestion, affinity-purified human 26S proteasomes from HEK293-PSMB2/β4-HB cells were subjected to the same trypsin treatment (Figure 1IB). Unlike the isolated EVs, both 20S subunits and 19S subunits in the purified proteasomes were completely digested. These results strongly suggest that the majority of 20S proteasomes are encapsulated within EVs rather than associated with the outer membrane of EVs. In contrast, the 19S complex (as singly-capped 26S or doubly-capped 30S proteasomes) appears to associate with the EV surface through weak, non-specific binding.

To assess the structural integrity of the EV-proteasomes, we used non-denaturing (native) PAGE and two methods to visualise the proteasomes: (1) in-gel hydrolysis of fluorogenic suc-LLVY-AMC (enzyme-substrate overlays) and (2) immunoblotting against the 20S subunit PSMA4 and the 19S subunit PSMC2 (Park et al. 2022). Both assays verified the presence of intact (functional) 26S and 30S holoenzymes in HEK293-PSMB2/β4-HB whole-cell lysates (WCLs; positive controls). In sharp contrast, no 26S proteasomes were found in the EVs isolated from the culture media (Figure 1G). After adding 0.02% SDS to the native gel to activate the 20S proteasome (Choi et al. 2023), both the WCLs and the EVs produced distinct proteasome activity (AMC fluorescence signals) corresponding to the 20S complex. Immunoblotting analysis confirmed these results: WCLs were positive for PSMA4 and PSMC2 from 26S and 20S proteasomes, respectively, whereas EVs showed only 20S signals (Figure 1G). We were unable to detect free 19S subcomplexes with the native gel/immunoblot analysis, suggesting their weak binding to EV membranes or their disassembly into individual subunits.

To further confirm that 20S proteasomes were encapsulated in EVs, we used affinity-purified 26S human proteasomes and ATP γ S, a non-hydrolysable ATP analogue, to stimulate their proteolytic activity. When ATP γ S binds to PSMC ATPases, it enhances the AAA ATPase activity of 26S proteasomes by causing structural rearrangements of the 19S complex from a substrate pre-engaged conformation to a translocation-competent one (Li and Demartino 2009). The suc-LLVY-AMC hydrolysis activity of purified 26S proteasomes (5 nM) from the HEK293-PSMB2/β4-HB cell line significantly increased in the presence of ATP γ S (1 µM) by ~2 fold (10,738 with ATP vs. 21,423 with ATP γ S during a 60-min reaction in a relative fluorescence unit [RFU]; $p < 0.05$ from one-way ANOVA followed by Bonferroni's post hoc test) (Figure 1IC). However, ATP γ S virtually did not affect EV-proteasome activity (6141 with ATP vs. 6582 with ATP γ S in RFU at 60 min; Figure 1IH), demonstrating that the encapsulated 20S, but not the 26S proteasome, is primarily involved in the proteasome activity observed in the isolated EVs. We also measured the proteolytic kinetics of EV-proteasomes using suc-LLVY-AMC and ATP γ S and found the V_{\max} values of EV proteasomes in the presence of ATP (9.86 nM/min) or ATP γ S (10.43 nM/min) were highly comparable (Figure 1I). Taken together, our findings suggest that 20S proteasomes, rather than 26S proteasomes, are packaged into the lumen of EVs and then released into the extracellular space.

3.3 | EV-Proteasomes Are Delivered to Recipient Cells

Previous studies have shown that EVs are involved in the distribution of a variety of proteins, including enzymes, antigens and transmembrane proteins (Chen et al. 2021); however, the delivery of proteasome-containing EVs and their impact on the recipient cell function have yet to be investigated. To evaluate whether 20S proteasomes can be delivered in EVs, we isolated EVs from the HEK293-PSMB2/β4-HB cells. This ensured that the majority of encapsulated 20S proteasomes were labelled with His tags (Choi, Yun et al. 2020). Next, we treated HEK293, A549 and SW480 cell lines with varying amounts of these EVs for 24 h before analysing WCLs from the target cells using immunoblotting. Our findings revealed a strong EV dose-dependent increase in PSMB2-His-positive band intensities in recipient cell lysates (Figure 2A–D), confirming that exogenous proteasomes could be delivered directly via EVs.

Furthermore, we investigated whether exogenous proteasomes delivered to target cells affected their overall proteasome activity. WCLs from the recipient cells were analysed for proteasome activity using suc-LLVY-AMC fluorescence and in-gel hydrolysis assays. These results revealed a mild but significant increase in cellular proteasome activity in response to the increased amounts of EVs (Figure 2B). However, we were unable to observe significant changes in the activity of either 20S or 26S proteasomes through non-denaturing (native) SDS-PAGE and in-gel substrate hydrolysis (Figure S2A). This cell-to-cell transmission appears to be achieved by direct fusion at the plasma membrane, independent of the endo-lysosomal pathway, because late endosome and lysosome makers, Rab7 and LAMP1 did not colocalise with internalised HB-tagged EV-proteasomes (Figure S2B).

Next, we investigated whether EV-proteasomes influenced the regulation of key protein homeostasis pathways in recipient cells. We found that endogenous proteasome substrates (p53 and Mcl-1), polyUb conjugates, the endo-lysosomal system (LAMP2, Rab5 and Rab7) and autophagy markers (p62 and lipidated LC3-II) were unaffected by EV treatment (Figure 2E). These results suggest that exogenous proteasomes do not cause widespread changes in the cellular proteome or related pathways. At the same time, we discovered that EV-proteasomes lowered the level of transiently overexpressed GFPu, a model substrate of cellular proteasomes, in the recipient cells (Figure 2F). These findings indicate that EV-mediated exogenous proteasome delivery may improve cellular proteasome activity while maintaining protein homeostasis, hence facilitating substrate degradation.

3.4 | EV-Proteasomes Facilitate the Degradation of Overexpressed Tau

Because EV-proteasomes isolated from culture media can be efficiently delivered to other cells, their effect on proteotoxic protein degradation was studied using the HEK293-derived doxycycline (Dox)-inducible human tau cell line (HEK293-TRex-tau40 cells), which expresses the longest isoform of human tau (2N4R) (Jiang et al. 2016). Dox concentration can precisely control tau expression and aggregation in this cell line (Figure S2C). To differentially induce tau expression, we treated the cells

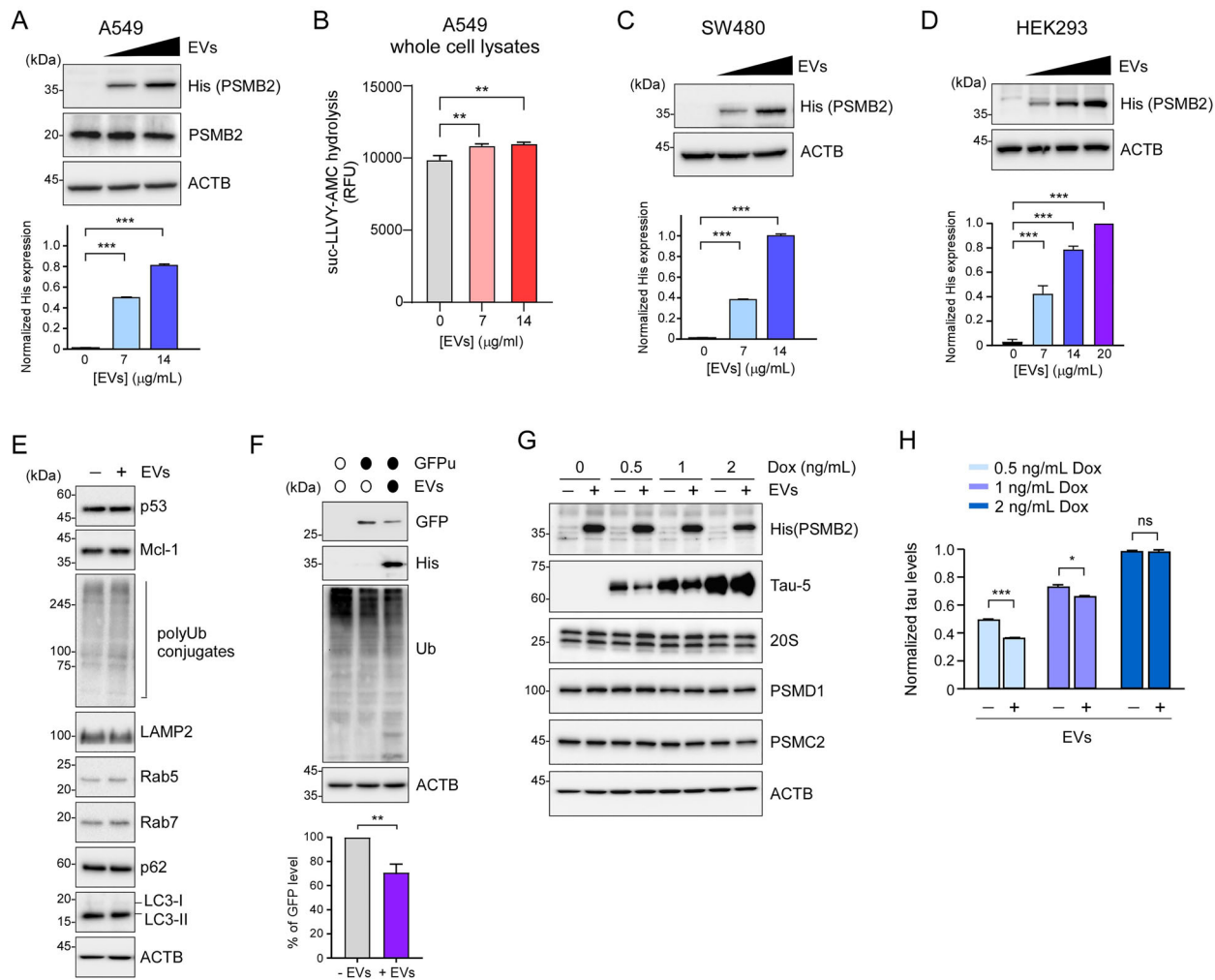


FIGURE 2 | Uptake of encapsulated EV-proteasomes by recipient cells and degradation of tau proteins by proteasomes encapsulated in EVs. (A) A549 cells were treated for 24 h with EVs (0, 7 and 14 μg/mL) isolated from HEK293-PSMB2/β4-HB cells. Whole-cell lysates (WCLs) were subjected to SDS-PAGE/IB with anti-His antibodies (targeting the His-tagged PSMB2 subunit of EV-proteasomes) and anti-PSMB2. For quantification, His-PSMB2 levels were normalised to those of endogenous β-actin/ACTB. Bars represent the mean ± SD of three independent experiments ($N = 3$); *** $p < 0.001$, one-way ANOVA followed by Bonferroni's post hoc test. (B) After treatment of EVs (0, 7, 14 μg/mL) in A549 cells for 24 h, WCLs were subjected to a proteasome activity assay using suc-LLVY-AMC for 60 min. Data are presented as the mean ± SD ($N = 3$); ** $p < 0.01$, one-way ANOVA, followed by Bonferroni's post hoc test. (C and D) Experiments were performed as described in (A) using SW480 (C) and HEK293 (D) cells. (E) HEK293 cells were treated with 60 μg/mL of 20S proteasome-containing EVs for 24 h. WCLs were prepared and subjected to SDS-PAGE/IB against endogenous proteins, including proteasome substrates (p53, Mcl-1), total ubiquitin (Ub), endosome-lysosome-associated proteins (LAMP2, Rab5, Rab7) and autophagy marker proteins (p62, LC3-I, LC3-II) to validate the maintenance of protein homeostasis. (F) Experiments were performed as described in (D) in cells transiently overexpressing GFPu, a fusion protein of the 16 amino acid degron CL1 and GFP, to examine the ability of EV-20S proteasomes to degrade the exogenous substrates. For quantification, signals from GFP were normalised to those of endogenous ACTB. Bars represent the mean ± SD; ** $p < 0.01$, unpaired Student's t -test. (G) HEK293-Trex-htau40 cells were treated with different concentrations of Dox (0, 0.5, 1 and 2 ng/mL) for 24 h, followed by EV-proteasome treatment (60 μg/mL) for an additional 24 h. WCLs were prepared and subjected to SDS-PAGE/IB against the indicated proteins to examine the uptake of EV-mediated 20S proteasome by the cells. (H) Levels of induced tau proteins were quantified and normalised to endogenous ACTB in (G). Each bar graph represents the mean ± SD; * $p < 0.05$, *** $p < 0.001$; one-way ANOVA followed by Bonferroni's post hoc test. ns, not significant.

with increasing doses of Dox (0, 0.5, 1 and 2 ng/mL) for 24 h, before adding enriched EV-proteasomes for another 24 h. The immunoblotting of WCLs revealed that tau protein levels were significantly reduced in the presence of EVs at 0.5 and 1 ng/mL Dox concentrations (Figure 2G,H); however, when excess tau was expressed with more than 2 ng/mL Dox, the effect of EV-proteasomes on tau levels was not apparent, implying that the levels of exogenous proteasomes were insufficient to process the excessive amounts of tau proteins in the cells. Collectively, these

results indicate that enhancing cellular proteasome activity via EV-proteasome delivery could be a feasible strategy for degrading disease-related proteotoxic proteins.

4 | Discussion

Cproteasomes have been found in the extracellular space, with increased concentrations observed in various diseases, but the

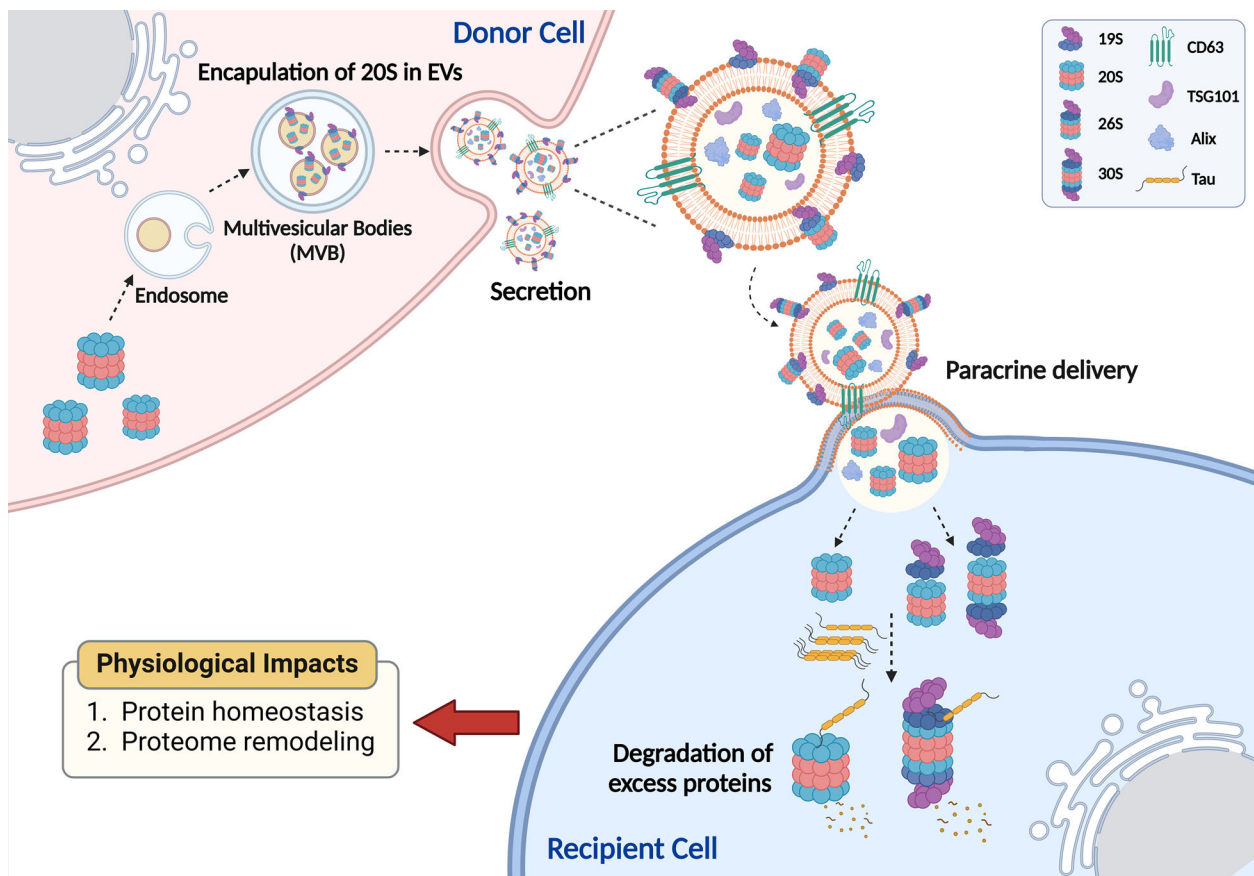


FIGURE 3 | Schematic illustration of the secretion and uptake of EV-encapsulated proteasomes.

Intracellular 20S proteasomes are packaged into EVs and secreted as an active, stand-alone protease complex. These EV-proteasomes are taken up by recipient cells, where they degrade excess substrates. This mechanism suggests a novel cell-to-cell communication system, which may contribute to protein homeostasis during proteotoxic stress or global proteome remodelling during cellular differentiation.

mechanisms underlying their secretion and action in ATP-depleted environments remain elusive. This extracellular distribution of c-proteasomes is not due to passive efflux or defective apoptosis of blood or endothelial cells, as there is no substantial correlation between c-proteasomes levels and cytolysis indicators (Stoebner et al. 2005; Lavabre-Bertrand et al. 2001). The findings of this study show that active 20S proteasomes were likely to be encapsulated into EV, instead of integrally or peripherally bound to EV membranes, under normal conditions, actively released into the extracellular space and could be taken up by recipient cells in a paracrine manner (Figure 3). The 26S proteasome could be associated with the external surface of EV membranes, but unlike 20S, they were highly sensitive to trypsin digestion (Figure 1F). Alternative proteasome activators, including PA28 $\alpha\beta$ /11S, PA28 γ and PA200, which function independently of ATP or ubiquitin, may be the cognate partners of the encapsulated 20S proteasome, affecting their biochemical functions (Bec et al. 2019).

The stand-alone 20S proteasome is more structurally stable and enzymatically active than the 26S counterpart in the oxidising extracellular space, as evidenced by its sustained activity in an ATP γ S-enriched setting (Figure 1H,I). Furthermore, only the 20S proteasome was detected using both native

PAGE/immunoblotting and in-gel activity assays (Figure 1G). At present, the sequence of events remains unclear; that is, does the disassembly event of 26S proteasomes into 20S and 19S subcomplexes precede their packaging process into EVs or do specific stressors and associated signalling pathways promote EV-proteasome biogenesis, thereby facilitating intercellular proteolytic communications? We postulate that cellular redox and metabolic states may influence the levels of secreted EV-proteasomes because oxidative stress and glucose deprivation are known to upregulate free 20S proteasomes in cells (Choi et al. 2023). Considering that proteasome activity in the EVs released by the apoptotic cells increased with vascular injury, the EV-proteasomes may represent an additional strategy of organisms for adaptive humoral responses, although their cellular origin and function remain largely unknown (Dieude et al. 2015). Given its substantial size (~ 120 Å in diameter and ~ 150 Å in height), the 20S proteasome is more likely to be encapsulated within larger EVs, such as ectosomes (100–350 nm in diameter), rather than smaller exosomes (50–100 nm) (Bec et al. 2019; Bochmann et al. 2014). However, the exact secretory pathway remains to be elucidated. No specific transporter has been identified for the direct export of such large complexes through the plasma membrane. Thus, EV-mediated secretion likely represents the primary route for extracellular proteasome release.

We also demonstrated that EVs could deliver exogenous proteasomes to target cells, promoting tau degradation (Figure 2G,H). These findings imply that the 20S proteasomes enclosed in EVs are capable of degrading intracellular proteins in recipient cells. It is also conceivable that exogenous 20S proteasomes may reassemble with endogenous 19S regulatory particles to form functional holoenzymes with expanded proteolytic capacities. Future studies should aim to explore the physiological relevance of this mechanism, particularly in processes involving large-scale proteome changes. For instance, we speculate that circulating EV-proteasomes may play a role in cellular differentiation, as observed during the transition from reticulocytes to erythrocytes—a context in which both proteasomes and exosomes were first identified in the 1980s (Johnstone et al. 1987; Hough et al. 1987). EV-mediated delivery of 20S proteasomes may be one of the cell-to-cell communication strategies for cells to respond severe proteotoxic stress. Upon uptake, these proteasomes may help degrade excess or pathological substrates, including tau, TDP-43 and other known aggregation-prone proteins, thereby reducing their intracellular levels. Our findings highlight the potential therapeutic implications of EV-proteasomes, especially in neurodegenerative diseases, as EVs are known to cross the blood–brain barrier (Wang et al. 2024; Ramos-Zaldivar et al. 2022). To sum up, major unresolved questions and our future research direction are on the biogenesis of EV-proteasomes, their cellular origin in organisms, the regulatory stimuli that cause their release, inter-cellular trafficking and propagation, and the consequences on recipient cell physiology. Genetically enhanced 20S proteasome activity and more efficient EV-producing cells could open up new therapeutic opportunities by enabling the delivery of therapeutic EV-proteasomes in vivo.

Author Contributions

Jiseong Kim: data curation (equal), formal analysis (equal), investigation (equal), methodology (equal), validation (equal), visualisation (equal), writing—original draft (equal). **Yuping Zhao:** data curation (equal), formal analysis (equal), investigation (equal), methodology (equal), validation (equal). **Hyun Young Kim:** formal analysis (supporting), methodology (supporting), resources (supporting). **Sumin Kim:** data curation (supporting), investigation (supporting), methodology (supporting). **Yanxialei Jiang:** funding acquisition (lead), investigation (lead), methodology (lead), supervision (lead), writing—original draft (equal), writing—review and editing (lead). **Min Jae Lee:** conceptualisation (lead), formal analysis (lead), funding acquisition (lead), investigation (lead), methodology (lead), project administration (lead), resources (lead), supervision (lead), writing—original draft (equal), writing—review and editing (lead).

Acknowledgements

This work was supported by grants from the National Research Foundation (NRF) of Korea (2020R1A5A1019023, RS-2021-NR059245 and RS-2023-00261784 to M.J.L.; RS-2024-00410687 to J.K.; 2022R1C1C2007752 to H.Y.K.), the Korea Health Industry Development Institute and Korea Dementia Research Centre (RS-2024-00332875 to M.J.L.) and the China Scholarship Council (202108370145 to Y.J.).

Conflicts of Interest

The authors declare no conflicts of interest.

Data Availability Statement

The data that support the findings of this study are available on request from the corresponding author.

References

- Abi Habib, J., E. De Plaen, V. Stroobant, et al. 2020. “Efficiency of the Four Proteasome Subtypes to Degrade Ubiquitinated or Oxidized Proteins.” *Scientific Reports* 10, no. 1: 15765.
- Andreu, Z., and M. Yáñez-Mó. 2014. “Tetraspanins in Extracellular Vesicle Formation and Function.” *Frontiers in Immunology* 5: 442.
- Bec, N., A. Bonhoure, L. Henry, et al. 2019. “Proteasome 19S RP and Translation Preinitiation Complexes Are Secreted Within Exosomes Upon Serum Starvation.” *Traffic (Copenhagen, Denmark)* 20, no. 7: 516–536.
- Ben-Nissan, G., N. Katzir, M. G. Füzesi-Levi, and M. Sharon. 2022. “Biology of the Extracellular Proteasome.” *Biomolecules* 12, no. 5: 619.
- Bochmann, I., F. Ebstein, A. Lehmann, et al. 2014. “T Lymphocytes Export Proteasomes by Way of Microparticles: A Possible Mechanism for Generation of Extracellular Proteasomes.” *Journal of Cellular and Molecular Medicine* 18, no. 1: 59–68.
- Byun, I., H. Seo, J. Kim, D. Jeong, D. Han, and M. J. Lee. 2023. “Purification and Characterization of Different Proteasome Species From Mammalian Cells.” *STAR Protocols* 4, no. 4: 102748.
- Chanda, D., E. Otoupalova, K. P. Hough, et al. 2019. “Fibronectin on the Surface of Extracellular Vesicles Mediates Fibroblast Invasion.” *American Journal of Respiratory Cell and Molecular Biology* 60, no. 3: 279–288.
- Chen, H., L. Wang, X. Zeng, et al. 2021. “Exosomes, a New Star for Targeted Delivery.” *Frontiers in Cell and Developmental Biology* 9: 751079.
- Choi, D., G. Go, D. K. Kim, et al. 2020. “Quantitative Proteomic Analysis of Trypsin-Treated Extracellular Vesicles to Identify the Real-Vesicular Proteins.” *Journal of Extracellular Vesicles* 9, no. 1: 1757209.
- Choi, W. H., S. A. de Poot, J. H. Lee, et al. 2016. “Open-Gate Mutants of the Mammalian Proteasome Show Enhanced Ubiquitin-Conjugate Degradation.” *Nature Communications* 7: 10963.
- Choi, W. H., S. Kim, S. Park, and M. J. Lee. 2021. “Concept and Application of Circulating Proteasomes.” *Experimental & Molecular Medicine* 53, no. 10: 1539–1546.
- Choi, W. H., Y. Yun, I. Byun, et al. 2023. “ECPAS/Ecm29-Mediated 26S Proteasome Disassembly Is an Adaptive Response to Glucose Starvation.” *Cell Reports* 42, no. 7: 112701.
- Choi, W. H., Y. Yun, S. Park, et al. 2020. “Aggresomal Sequestration and STUB1-Mediated Ubiquitylation During Mammalian Proteophagy of Inhibited Proteasomes.” *PNAS* 117, no. 32: 19190–19200.
- Dieude, M., C. Bell, J. Turgeon, et al. 2015. “The 20S Proteasome Core, Active Within Apoptotic Exosome-Like Vesicles, Induces Autoantibody Production and Accelerates Rejection.” *Science Translational Medicine* 7, no. 318: 318ra200.
- Dwivedi, V., K. Yaniv, and M. Sharon. 2021. “Beyond Cells: The Extracellular Circulating 20S Proteasomes.” *Biochimica et Biophysica Acta - Molecular Basis of Disease* 1867, no. 3: 166041.
- EL Andaloussi, S., I. Mäger, X. O. Breakefield, and M. J. Wood. 2013. “Extracellular Vesicles: Biology and Emerging Therapeutic Opportunities.” *Nature Reviews Drug Discovery* 12, no. 5: 347–357.
- Fabre, B., T. Lambour, L. Garrigues, et al. 2014. “Label-Free Quantitative Proteomics Reveals the Dynamics of Proteasome Complexes Composition and Stoichiometry in a Wide Range of human Cell Lines.” *Journal of Proteome Research* 13, no. 6: 3027–3037.
- Finley, D., X. Chen, and K. J. Walters. 2016. “Gates, Channels, and Switches: Elements of the Proteasome Machine.” *Trends in Biochemical Sciences* 41, no. 1: 77–93.
- Gardiner, C., D. Di Vizio, S. Sahoo, et al. 2016. “Techniques Used for the Isolation and Characterization of Extracellular Vesicles: Results of a Worldwide Survey.” *Journal of Extracellular Vesicles* 5: 32945.

- Herrmann, I. K., M. J. A. Wood, and G. Fuhrmann. 2021. "Extracellular Vesicles as a Next-Generation Drug Delivery Platform." *Nature Nanotechnology* 16, no. 7: 748–759.
- Hough, R., G. Pratt, and M. Rechsteiner. 1987. "Purification of Two High Molecular Weight Proteases From Rabbit Reticulocyte Lysate." *Journal of Biological Chemistry* 262, no. 17: 8303–8313.
- Jiang, Y., J. Lee, J. H. Lee, et al. 2016. "The Arginylation Branch of the N-End Rule Pathway Positively Regulates Cellular Autophagic Flux and Clearance of Proteotoxic Proteins." *Autophagy* 12, no. 11: 2197–2212.
- Johnstone, R. M., M. Adam, J. R. Hammond, L. Orr, and C. Turbide. 1987. "Vesicle Formation During Reticulocyte Maturation. Association of Plasma Membrane Activities With Released Vesicles (exosomes)." *Journal of Biological Chemistry* 262, no. 19: 9412–9420.
- Kim, S., S. H. Park, W. H. Choi, and M. J. Lee. 2022. "Evaluation of Immunoproteasome-Specific Proteolytic Activity Using Fluorogenic Peptide Substrates." *Immune Network* 22, no. 3: e28.
- Kostallari, E., S. Valainathan, L. Biquard, V. H. Shah, and P. E. Rautou. 2021. "Role of Extracellular Vesicles in Liver Diseases and Their Therapeutic Potential." *Advanced Drug Delivery Reviews* 175: 113816.
- Lavabre-Bertrand, T., L. Henry, S. Carillo, et al. 2001. "Plasma Proteasome Level Is a Potential Marker in Patients With Solid Tumors and Hemopoietic Malignancies." *Cancer: Interdisciplinary International Journal of the American Cancer Society* 92, no. 10: 2493–2500.
- Lehrich, B. M., Y. Liang, and M. S. Fiandaca. 2021. "Foetal Bovine Serum Influence on in Vitro Extracellular Vesicle Analyses." *Journal of Extracellular Vesicles* 10, no. 3: e12061.
- Li, X., and G. N. Demartino. 2009. "Variably Modulated Gating of the 26S Proteasome by ATP and Polyubiquitin." *Biochemical Journal* 421, no. 3: 397–404.
- Lim, Y., H. Y. Kim, D. Han, and B. K. Choi. 2023. "Proteome and Immune Responses of Extracellular Vesicles Derived From Macrophages Infected With the Periodontal Pathogen *Tannerella forsythia*." *Journal of Extracellular Vesicles* 12, no. 12: e12381.
- Lobb, R. J., M. Becker, S. W. Wen, et al. 2015. "Optimized Exosome Isolation Protocol for Cell Culture Supernatant and Human Plasma." *Journal of Extracellular Vesicles* 4, no. 1: 27031.
- Mathieu, M., L. Martin-Jaular, G. Lavieu, and C. Théry. 2019. "Specificities of Secretion and Uptake of Exosomes and Other Extracellular Vesicles for Cell-to-Cell Communication." *Nature Cell Biology* 21, no. 1: 9–17.
- Mathieu, M., N. Névo, M. Jouve, et al. 2021. "Specificities of Exosome Versus Small Ectosome Secretion Revealed by Live Intracellular Tracking of CD63 and CD9." *Nature Communications* 12, no. 1: 4389.
- Matyskiela, M. E., G. C. Lander, and A. Martin. 2013. "Conformational Switching of the 26S Proteasome Enables Substrate Degradation." *Nature Structural & Molecular Biology* 20, no. 7: 781–788.
- Murphy, D. E., O. G. de Jong, M. J. W. Evers, M. Nurazizah, R. M. Schiffelers, and P. Vader. 2021. "Natural or Synthetic RNA Delivery: A Stoichiometric Comparison of Extracellular Vesicles and Synthetic Nanoparticles." *Nano Letters* 21, no. 4: 1888–1895.
- Park, S. H., W. H. Choi, and M. J. Lee. 2022. "Effects of mTORC1 Inhibition on Proteasome Activity and Levels." *BMB Reports* 55, no. 4: 161–165.
- Patel, G. K., M. A. Khan, H. Zubair, et al. 2019. "Comparative Analysis of Exosome Isolation Methods Using Culture Supernatant for Optimum Yield, Purity and Downstream Applications." *Scientific Reports* 9, no. 1: 5335.
- Piffoux, M., A. K. A. Silva, J. B. Lugagne, P. Hersen, C. Wilhelm, and F. Gazeau. 2017. "Extracellular Vesicle Production Loaded With Nanoparticles and Drugs in a Trade-Off Between Loading, Yield and Purity: Towards a Personalized Drug Delivery System." *Advanced Biosystems* 1, no. 5: e1700044.
- Rackov, G., N. Garcia-Romero, S. Esteban-Rubio, J. Carrión-Navarro, C. Belda-Iniesta, and A. Ayuso-Sacido. 2018. "Vesicle-Mediated Control of Cell Function: The Role of Extracellular Matrix and Microenvironment." *Frontiers in Physiology* 9: 651.
- Rajkumar, S. V., M. A. Dimopoulos, A. Palumbo, et al. 2014. "International Myeloma Working Group Updated Criteria for the Diagnosis of Multiple Myeloma." *Lancet Oncology* 15, no. 12: e538–e548.
- Ramos-Zaldivar, H. M., I. Polakovicova, E. Salas-Huenuleo, et al. 2022. "Extracellular Vesicles Through the Blood-Brain Barrier: A Review." *Fluids Barriers CNS* 19, no. 1: 60.
- Rider, M. A., S. N. Hurwitz, and D. G. Meckes Jr. 2016. "ExtraPEG: A Polyethylene Glycol-Based Method for Enrichment of Extracellular Vesicles." *Scientific Reports* 6: 23978.
- Sledz, P., P. Unverdorben, F. Beck, et al. 2013. "Structure of the 26S Proteasome With ATP-gammaS Bound Provides Insights Into the Mechanism of Nucleotide-Dependent Substrate Translocation." *PNAS* 110, no. 18: 7264–7269.
- Stoebner, P.-E., T. Lavabre-Bertrand, L. Henry, et al. 2005. "High Plasma Proteasome Levels Are Detected in Patients With Metastatic Malignant Melanoma." *British Journal of Dermatology* 152, no. 5: 948–953.
- Théry, C., K. W. Witwer, E. Aikawa, et al. 2018. "Minimal Information for Studies of Extracellular Vesicles 2018 (MISEV2018): A Position Statement of the International Society for Extracellular Vesicles and Update of the MISEV2014 Guidelines." *Journal of Extracellular Vesicles* 7, no. 1: 1535750.
- Turker, F., E. K. Cook, and S. S. Margolis. 2021. "The Proteasome and Its Role in the Nervous System." *Cell Chemical Biology* 28, no. 7: 903–917.
- Wang, W., H. Sun, H. Duan, et al. 2024. "Isolation and Usage of Exosomes in Central Nervous System Diseases." *CNS Neuroscience & Therapeutics* 30, no. 3: e14677.
- Wu, W. C., S. J. Song, Y. Zhang, and X. Li. 2020. "Role of Extracellular Vesicles in Autoimmune Pathogenesis." *Frontiers in Immunology* 11: 579043.
- Yun, Y., S. Y. Lee, W. H. Choi, et al. 2020. "Proteasome Activity in the Plasma as a Novel Biomarker in Mild Cognitive Impairment With Chronic Tinnitus." *Journal of Alzheimer's Disease* 78, no. 1: 195–205.

Supporting Information

Additional supporting information can be found online in the Supporting Information section.